Ultrasonics Sonochemistry 95 (2023) 106360

Contents lists available at ScienceDirect

Ultrasonics Sonochemistry

journal homepage: www.elsevier.com/locate/ultson

Ultrasound-assisted Peptide Nucleic Acids synthesis (US-PNAS)

Alessandra Del Bene [a], Antonia D'Aniello [a], Stefano Tomassi [b], Francesco Merlino [b], Vincenzo Mazzarella [a], Rosita Russo [a], Angela Chambery [a], Sandro Cosconati [a], Salvatore Di Maro [a,*], Anna Messere [a,*]

[a] Department of Environmental, Biological and Pharmaceutical Science and Technology, University of Campania "Luigi Vanvitelli", 81100 Caserta, Italy
[b] Department of Pharmacy, University of Naples "Federico II", 80131 Naples, Italy

ARTICLE INFO

Keywords:
Peptide Nucleic Acid
Ultrasonication
Sonochemistry
Solid-Phase Synthesis
Coupling Conditions

ABSTRACT

Herein, we developed an innovative and easily accessible solid-phase synthetic protocol for Peptide Nucleic Acid (PNA) oligomers by systematically investigating the ultrasonication effects in all steps of the PNA synthesis (US-PNAS). When compared with standard protocols, the application of the so-obtained US-PNAS approach succeeded in improving the crude product purities and the isolated yields of different PNA, including small or medium-sized oligomers (5-mer and 9-mer), complex purine-rich sequences (like a 5-mer Guanine homoligomer and the telomeric sequence TEL-13) and longer oligomers (such as the 18-mer anti-IVS2-654 PNA and the 23-mer anti-mRNA 155 PNA). Noteworthy, our ultrasound-assisted strategy is compatible with the commercially available PNA monomers and well-established coupling reagents and only requires the use of an ultrasonic bath, which is a simple equipment generally available in most synthetic laboratories.

1. Introduction

Since 1991, when Nielsen *et al.* reported the first polyamide nucleic acid oligomer [1], Peptide Nucleic Acids (PNA) have made their way in different fields, including but not limited to chemistry, molecular and cell biology, drug discovery and diagnostics [2]. PNA are artificial DNA-like molecules endowed with an uncharged peptidomimetic backbone consisting of nucleobases-functionalized N-(2-aminoethyl) glycine (AEG) units in place of the sugar-phosphodiester moieties [1,3] (Fig. 1).

Single-stranded PNA are endowed with numerous favorable properties, such as high thermal and metabolic stability, strong and fast binding affinity to the complementary nucleic acid, and high sensitivity to a single mismatch, which have drawn great attention from the nucleic acid scientific community [4,5]. Particularly, they have been successfully employed as diagnostic tools at the interface of chemistry and biology for genetic diagnosis, cytogenetics, and pharmaceutical applications [6]. In biomedical applications, PNA emerged as potential therapeutics in antigene [7] and antisense [8] approaches, as anticancer [9], as antibiotics for treating multidrug-resistant infections [10,11], as antiviral for efficiently inhibiting the viral replication processes [7,12]. PNA are also used as probes in place of DNA in various investigative procedures [6], including *in-vitro* assays, chromosomal analysis, Polymerase Chain Reaction (PCR), *in-vivo* imaging, and Fluorescence *In Situ* Hybridization (PNA-FISH). Additional applications are the development of PNA-encoded libraries, PNA-based photosensitive compounds, and PNA microarrays. Unfortunately, the translation of the PNA potential in preclinical and clinical contexts has revealed serious limits, like their poor cell permeability, low aqueous solubility, and the sequence-dependent self-aggregation phenomenon [17], which have been handled by exploring several chemical strategies [13–17]. A large number of modifications of the canonical PNA structure has been reported, [17] including but not limited to chiral, cyclic, and locked PNA. However, most biological studies and applications involving PNA still employ the classical AEG-based PNA, probably as a consequence of their favorable nucleic acid binding properties and high chemical and biological stability. Thus, the continuous evolution of PNA-based applications supports the endless pursuit of faster and improved synthetic methods for PNA oligomers. Solid Phase Synthesis (SPS) unambiguously represents the most efficient approach for synthesizing oligomers with high purity and good yields. Numerous orthogonal protecting strategies for the PNA monomers have been proposed (e.g. Boc/Cbz, Fmoc/Cbz, Fmoc/Boc, and Fmoc/Bhoc) [18–24] for temporarily protecting the backbone amine while preserving the stability of the exocyclic amine-protecting groups of the nucleobases. To date, most of the available

* Corresponding authors.
E-mail addresses: salvatore.dimaro@unicampania.it (S. Di Maro), anna.messere@unicampania.it (A. Messere).

https://doi.org/10.1016/j.ultsonch.2023.106360
Received 21 December 2022; Received in revised form 23 February 2023; Accepted 3 March 2023
Available online 8 March 2023

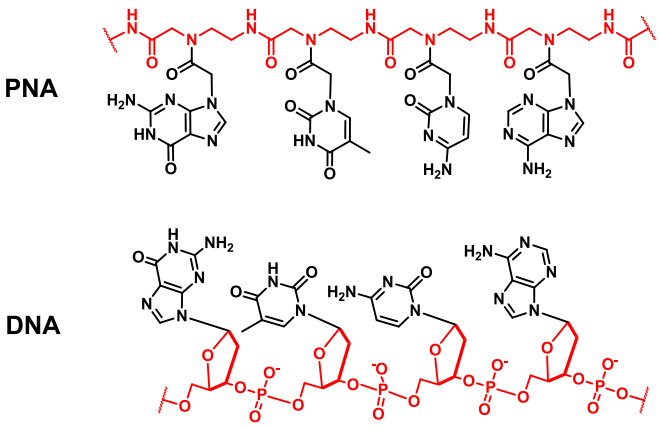

Fig. 1. Representative comparison between the structures of PNA and DNA fragments. The different DNA and PNA backbones are highlighted in red. (For interpretation of the references to colour in this figure legend, the reader is referred to the web version of this article.)

PNA monomers are marketed as Fmoc/Bhoc and Boc/Cbz. The latter is especially used for manual assembly of PNA oligomers, being the hydrofluoric-mediated deprotection conditions of Cbz groups unsuitable with the instrument metal parts of the automated synthesizers. On the other hand, Fmoc/Bhoc monomers have emerged as "gold standard" building blocks mostly employed in both automated and manual synthesis of PNA oligomers. Nowadays, automated solid-phase PNA synthesis is usually performed on conventional or μW-assisted synthesizers [25], according to standard protocols. The assembly of PNA oligomers by manual procedures derives from the same protocols developed for automated synthesis by Egholm and Casale [26] and depends on the reagent excesses, the reaction times, the oligomer sequence and length, and the operating temperature. Despite the significant progress achieved, PNA synthesis is still affected by numerous issues, such as the unsatisfied coupling yields in sequences endowed with a high content of sterically hindered purines. In particular, when Fmoc-protected monomers are employed, the growth of the purine-rich sequences is prevented by the stacking of the Fmoc group with the nucleobases and the aggregation of PNA chains on the solid support. Additionally, undesired side-reactions may occur during PNA syntheses, such as the N-acyl migration of the nucleobases with the formation of an abasic site (Fig. 2A) and the cyclization/elimination of monoketopiperazine, which involve the free terminal amine during the base-mediated deprotection (Fig. 2 B). Although deprotection times are generally very short in automatic and microwave syntheses, longer reaction times are required in manual synthesis and higher base-catalyzed rearrangements may occur.

Various strategies have been investigated to overcome these issues, including the modification of nucleobase protecting groups, solid supports, coupling reagents, and deprotection conditions [27–31], which have succeeded in enhancing the quality of PNA oligomers ranging from 10- to 15-mer. More recently, click ligation [32] and automated flow-based synthesis [33] have been settled to synthesize longer PNA-peptide conjugates.

In line with these studies, our and other teams have recently [34–39] reported the development of an ultrasound-assisted Solid Phase Peptide Synthesis strategy (US-SPPS) that enhanced the synthesis of different biologically active and difficult peptides without increasing the main side reactions, such as the aspartimide formation and the amino acid racemization. The use of ultrasounds in chemistry has received notable attention [40–43], due to their well-documented ability to enhance the reaction rates and the product yields in both heterogeneous and homogenous systems. These effects are mainly due to the cavitation phenomenon, in which the bubbles generated upon ultrasonic wave propagation in the fluid reach an unstable size and collapse, producing a dramatic local increment of temperature and pressure. In SPPS, direct use of ultrasounds afforded superior results when compared to standard protocols. Inspired by these results, we propose an unprecedent and easily accessible synthetic protocol for PNA oligomers, including purine-rich and long sequences, by employing ultrasonication in all the steps of the PNA synthesis (Fig. 3) (US-PNAS).

To date, no investigation has been carried out on the effect of ultrasonic waves in the solid-phase synthesis of PNA oligomers. The results of the present study provide evidence that the combination of ultrasonication with standard coupling agents and commercially available Fmoc/Bhoc-protected PNA monomers, leads to oligos with higher purity compared to traditional manual PNA synthesis.

2. Results and discussion

To develop an efficient ultrasound-assisted synthetic protocol for PNA by Fmoc/Bhoc chemistry, we preliminary screened different coupling reagents by synthesizing a model 5-mer PNA oligomer (Fmoc-TGACT-K-NH_2), containing all four nucleobases with a percentage of purines of 40% and a Lysine at C terminus, on a standard Rink Amide AM resin LL resin as solid support. The performance of each coupling strategy with Fmoc/Bhoc-protected monomers was evaluated by comparing the purity of the crude products and isolated yields obtained

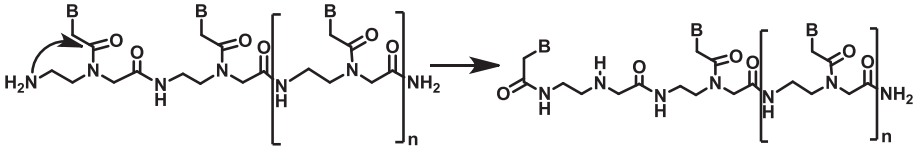

A: N-acyl transfer of the nucleobases leading to an abasic site

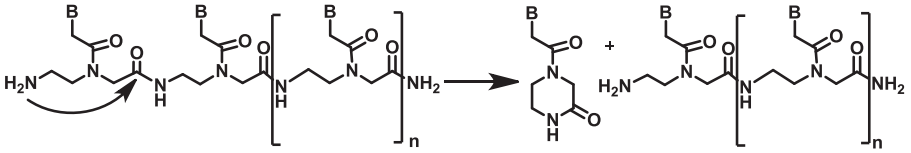

B: Cyclization leading to N-1 deletion sequences

Fig. 2. Undesired side-reactions during manual PNA synthesis (A: N-Acyl transfer; B: cyclization).

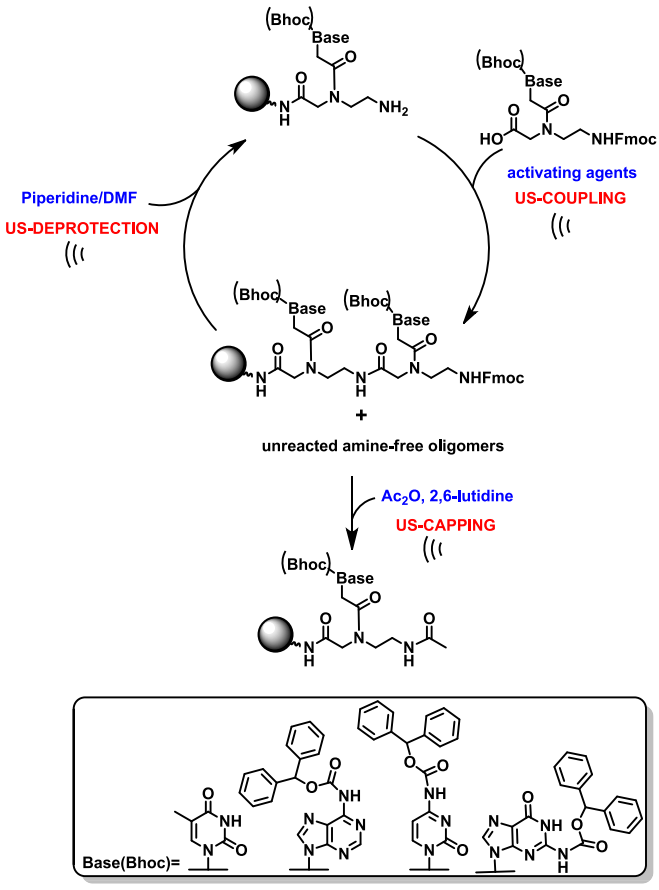

Fig. 3. General synthetic scheme for the proposed ultrasound-assisted Solid Phase Peptide Nucleic Acids strategy (US-PNAS).

by US-PNAS with those achieved with the standard protocol, consisting of 30 min reaction at room temperature with 5 equiv of PNA monomer in the presence of ((1-[bis(dimethylamino)methylene]-1H-1,2,3-triazolo [4,5-b]-pyridinium 3-oxide hexafluorophosphate) (HATU) and 2,6-lutidine (see Table S1 in supplementary material for isolated yields comparison). For this study, we selected some representative coupling strategies (Fig. 4) including DIC/Oxyma combination (N,N'-Diisopropylcarbodiimide/ethyl cyanohydroxyiminoacetate), HBTU (2-(1H-benzotriazol-1-yl)-1,1,3,3-tetramethyluronium hexafluorophosphate), PyAOP (7-azabenzo-triazol-1-yloxy)tripyrrolidinophosphonium hexafluorophosphate), HATU and COMU ((1-cyano-2-ethoxy-2-oxoethylidenaminooxy)-dimethylamino-morpholino-carbenium hexafluorophosphate).

The model PNA sequences were assembled by first varying the stoichiometry of reagents and then the coupling times. For all the syntheses, the deprotection time was fixed at 1 + 0.5 min and the capping time at 3 min, according to our previous studies on peptide synthesis [34]. For the coupling investigation, we set 5- and 10-min reaction times and used 5 equiv of each reactant, which is the same excess generally adopted for standard synthetic protocols. As depicted in Fig. 5, at 10 min coupling time, the ultrasonication did not generate any significant undesired products, including the formation of N-terminal tetramethylguanidinium by-products [44]. HATU, PyAOP and HBTU exhibited the highest percentages in terms of crude purity (in the range 63–72%) which were higher or comparable to the synthesis carried out by standard protocol (≈62%) (Figs. 5 and 6). The results of these first experiments led us to exclude from further investigations both DIC/Oxyma and COMU strategies, whose application produced unsatisfied results (37% and 44% crude purity, respectively). Noteworthy, the advantages of our strategy were confirmed by comparing the isolated yields of the 5-mer PNA obtained by the best US-assisted (52% isolated yield, Table S1 in supplementary material) and the standard protocol (36% isolated yield, Table S1 in supplementary material).

Considering that the PNA synthesis performance could be affected by the ultrasound-induced increment of temperature during the coupling steps and that the maximum temperature reached with a similar ultrasonic bath was 45 °C [34], to assess whether the observed improvement of the coupling yields could be ascribed to the sole temperature effect, the 5-mer was also synthesized by mechanical shaking at 45 °C, with a coupling time of 10 min. Noteworthy, we noticed a difference of about 20% purity comparing the sequences assembled by standard heating at 45 °C and with ultrasonication (entries 11 and 12 in Figs. 5 and 6), which indicated that the latter mainly accounts for the observed synthetic improvements.

At this stage, we selected 10 min and HATU, PyAOP, and HBTU as the best reaction condition and proceeded by decreasing the coupling/additive reagent and PNA monomer excess to 4, 3, and 2 equiv. As

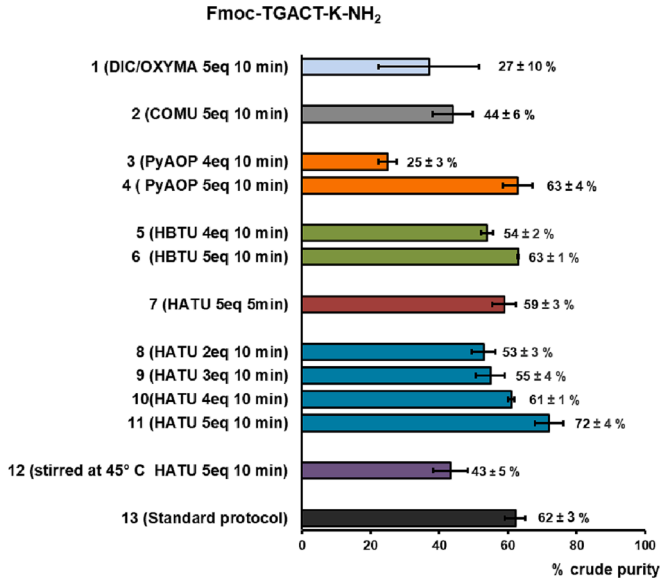

Fig. 5. Optimization study for the US-PNAS of the model 5-mer PNA oligomer (Fmoc-TGACT-K-NH_2). PNA synthesis was attained in triplicate and the resulting crude purities are expressed as a percentage (mean values ± standard error of measurement (SEM), N = 3).

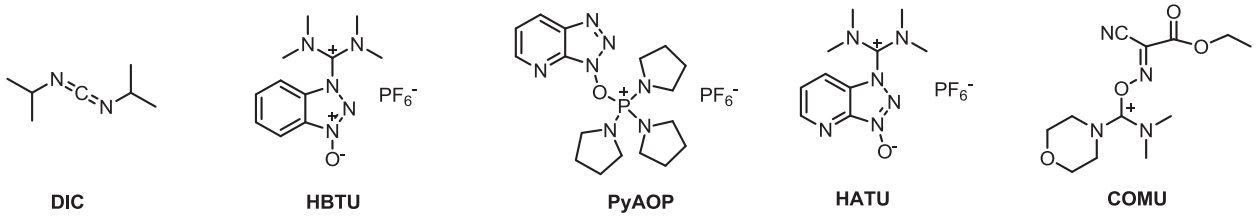

Fig. 4. Coupling agents screened in the US-PNAS oligomerization experiments.

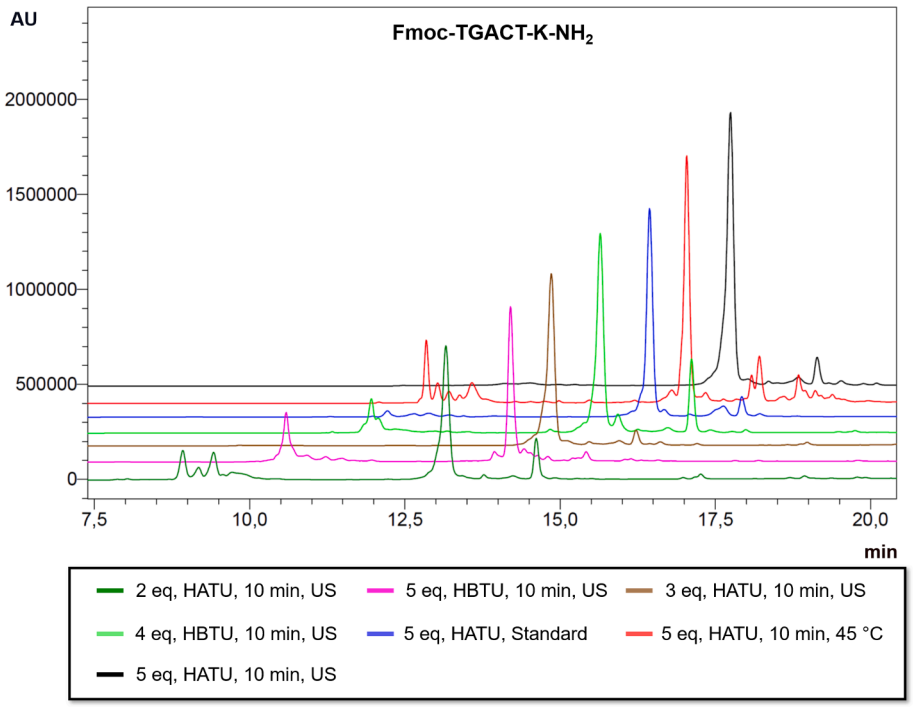

Fig. 6. Comparison of representative HPLC profiles of synthetic crudes of the model 5-mer PNA oligomer (Fmoc-TGACT-K-NH_2). Coupling reagents and synthetic methods are indicated. The crude purity was calculated by integrating the peaks at t_R = 13.15 min [analytical HPLC gradient 1 in HPLC and Mass spectrometry procedures section].

depicted in Fig. 5, the reduction of the reagent excesses generally affected the efficiency of the synthesis, with HATU performing much better than PyAOP and HBTU already at 4 equiv (≈25% and ≈54% for PyAOP and HBTU, respectively, compared to 60% for HATU). These results pointed out that the HATU is the best coupling agent among the tested ones for US-PNAS, providing suitable purity of crudes even at lower stoichiometric excesses (in the range of 61–53%) (entries 8, 9 and 10 in Figs. 5 and 6).

In light of these results, the US conditions comprising 5- and 10-min reaction times and 5 equiv reagent excess were exploited for the synthesis of a longer oligomer, 9-mer with a 33% purines content (H-TACACTGTC-K-NH_2) and compared to standard methods (Figs. 7 and 8).

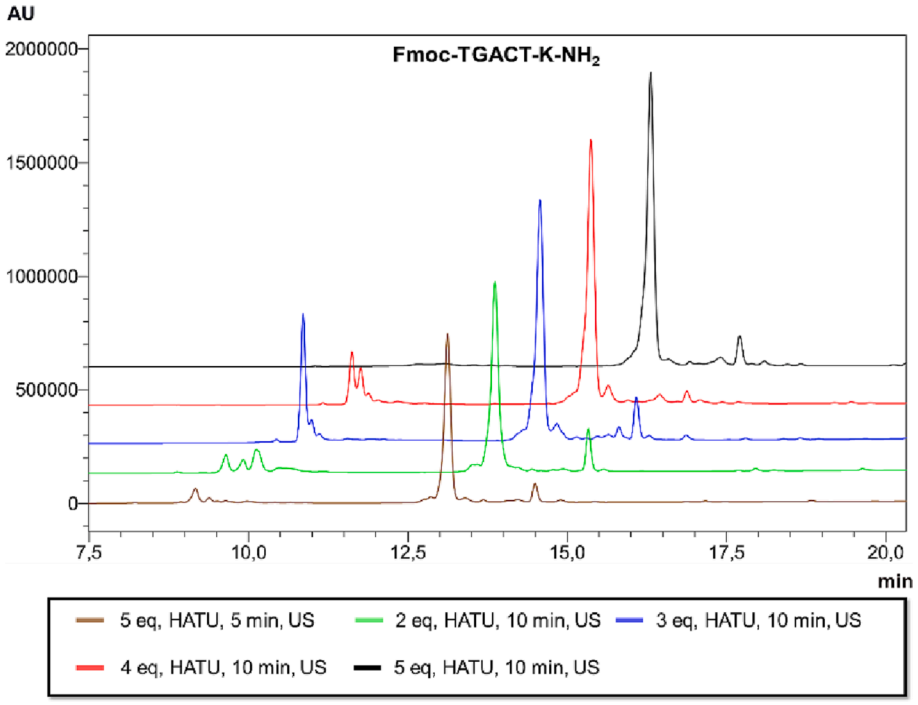

Fig. 7. Comparison of representative HPLC profiles of synthetic crudes of the model 5-mer PNA oligomer (Fmoc-TGACT-K-NH_2). Equivalents of reagents and reaction times are indicated. The crude purity was calculated by integrating the peaks at t_R = 13.15 min [analytical HPLC gradient 1 in HPLC and Mass spectrometry procedures section].

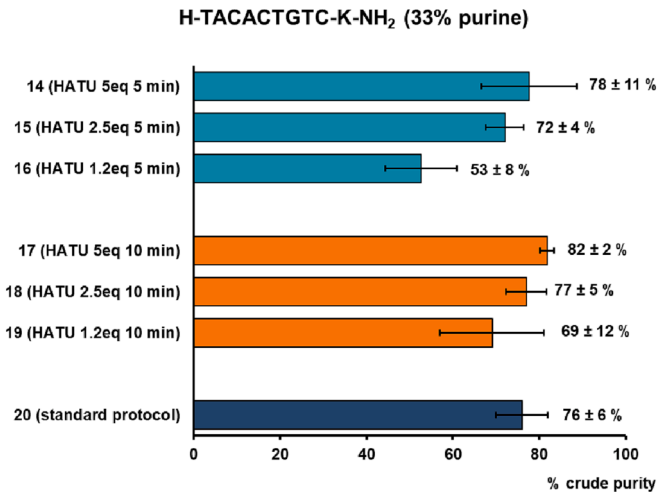

Fig. 8. Optimization study for the US-PNAS of the model 9-mer PNA oligomer (H-TACATGTC-K-NH_2). PNA synthesis was attained in triplicate and the resulting crude purities are expressed as a percentage (mean values ± standard error of measurement (SEM), N = 3).

As expected, when the purine percentage in the sequence decreased a higher efficiency of synthesis was observed with both standard (76 %) and US (>82 and 78 %) protocols (Fig. 8). However, we noticed a significative difference in terms of isolated yields comparing the US-assisted and the standard protocols (75 % vs 40 % isolated yields, Table S1 in supplementary material). In the successive set of experiments, both the reaction times (10 and 5 min) we employed and the excess of PNA monomer and HATU were reduced from 5 to 2.5 and 1.2 equiv to find the minimum reagents excess and reaction time for achieving the highest purity of the model 9-mer PNA oligomer. (See Fig. 9.)

As depicted in the HPLC analysis, both 10 and 5 min were appropriate coupling times when 5 equiv reagent excesses were used. Thus, these protocols were assessed for the synthesis of an additional 13-mer oligomer, characterized by a higher purine content, especially guanine. The 13-mer PNA, here referred to as TEL-13, has the sequence targeting the RNA subunit of telomerase, hTR [45]. Unfortunately, the assembly of TEL-13 PNA (H-CAGTTAGGGTTAG-K-NH_2) using HATU activation, with 5 equiv of reagents excess and 5 min coupling time afforded inadequate crude purity (≈23% see Table S1 in supplementary material) as judged by HPLC profile. Conversely, when the same was applied for longer coupling times (10 min) a significant increment of crude purity was observed (from ≈23% to ≈59%) (Fig. 10). Noteworthy, this US-assisted protocol (entry 22, Fig. 10) was also superior in terms of crude purity and isolated yields (see Table S1 in supplementary material) compared to the double coupling protocol. In addition, the crude HPLC profile of the not-irradiated manual synthesis of TEL13 PNA, exhibited side products as highlighted by the presence of a shoulder in the peak at 9.66 min (Fig. 10).

Finally, the efficiency of the best US-PNAS protocol (5 equiv reagent excess, 10 min reaction time, ultrasound-assisted) was compared to standard protocol by assembling additional PNA sequences, including the 5-mer PNA containing 100% guanine monomers as representative of a difficult sequence, the 18-mer anti-IVS2-654 PNA [33] and the 23-mer anti-miR-155 PNA as representative of longer sequences [46].

As depicted in Fig. 11, the 5-mer (Fmoc-GGGGG-NH_2), the 18-mer (H-AEEA-TTGGTTGGTTTGTTACCT-NH_2) and the anti-miR-155 PNA sequences (H-KKK-ACCCCTATCACAATTAGCATTAA-Gly-NH_2 and H-AEEA-ACCCCTATCACAATTA GCATTAA-Gly-NH_2) [46,47], were rapidly and successfully synthesized, resulting in final crude oligomers with purity (≈ 73 % for the 5-mer, ≈ 91% for the 18-mer oligomer and ≈ 68 %, ≈ 67 % for the two 23-mer oligomers) significantly higher compared to standard protocols (≈ 59 % for the 5-mer oligomer, ≈61% for the 18-mer and traces for the 23-mer oligomers) (see supporting material for HPLC profile and isolated yields comparison).

3. Conclusions and outlook

This study describes a new fast and efficient strategy for manual PNA synthesis based on the use of ultrasonication in each step of the synthetic procedure, which could complement or enhance the efficiency of the available manual or automatic protocols. Indeed, we demonstrated that the systematic use of ultrasounds during PNA synthesis improved the crude product purities of small or medium-sized oligomers (5-mer and 9-mer), of complex purine-rich sequences (like a 5-mer Guanine homo-oligomer and the telomeric sequence TEL-13) and longer oligomers (such as the 18-mer anti-IVS2-654 PNA, and the 23-mer anti-mRNA 155 PNA) without exacerbating the main side reactions. In light of these results, US-PNAS is a powerful method that fits with the commercially available PNA monomers and coupling reagents (HATU) and that only requires the use of an ultrasonic bath, a simple and accessible equipment generally found in most synthetic laboratories. We envisage that additional studies on a larger number of sequences will set the stage to define guidelines for optimized synthetic protocols suitable for oligomers with different length and nucleobase composition (for instance, 5 min coupling time and 1.2 reagent equiv for small oligomers with purine poor sequences). Encouraged by the results herein described, we are currently evaluating if US-PNAS might also be extended to the PNA analogs (e.g. γ-GPNA [48], bimodal PNA [49,50], PNA-like scaffolds [51]) endowed with more favourable physiochemical and biological properties but requiring more complex and/or cumbersome synthesis.

4. Materials and methods

The ultrasonic bath employed for this study was a SONOREX RK 52H by BANDELIN electronic (Germany), with internal dimensions of 150 × 140 × 100 mm and an operating volume of 1.2 L. The ultrasonic bath was equipped with timer control for 1–15 min, continuous (∞) operations, and built-in heating control (30–80 °C thermostatically adjustable). The ultrasonic frequency is 35 kHz. The ultrasonic nominal output is 60 W. The ultrasonic peak output is 240 W, corresponding to 4 times the ultrasonic nominal output. The heating power was 140 W.

Fmoc-PNA-T-OH, Fmoc-PNA-C(Bhoc)–OH, Fmoc-PNA-A(Bhoc)–OH, Fmoc-PNA-G(Bhoc)–OH (purity 95%) were all purchased from ASM Research Chemicals GmbH & Co. KG (Burgwedel, NDS, DE).

Fmoc-L-Lys(Boc)–OH, Fmoc-Gly, and Fmoc-AEAA-OH Spacer were from AAPPTec (Louisville, USA). Piperidine (peptide grade, purity 99.9 %), TFA (peptide grade, purity 99.9%), m-cresol, and N,N-diisopropylethylamine (DIPEA) (purity 99.7 %) were purchased from Iris-Biotech GmbH (Marktredwitz, Germany).

Coupling reagents such as HATU, HBTU (purity ≥ 98.0 %), HOBt (purity > 97 % dry weight, water ~ 12%), DIC (purity 99 %), PyAOP, COMU (purity 97 %), Oxyma (purity 97 %), were purchased by Sigma-Aldrich/Merck (St. Louis, USA). Acetic anhydride (Ac_2O, purity > 98 %), and 2,6-Lutidine (purity ≥ 96%) were purchased by Sigma-Aldrich Chemie GmbH (Buchs, Svizzera). The Rink Amide AM resin LL (0.2–0.4 mmol/g, 100–200 mesh) Novabiochem and Chem Matrix were purchased by Sigma-Aldrich Chemie GmbH (Buchs, Svizzera), and the manufacturer's reported loading of the resin was used in the calculations. Solvents for peptide synthesis and analysis such as N,N-dimethylformamide (DMF), dichloromethane (DCM), dimethyl sulfoxide (DMSO), water and acetonitrile (MeCN) for HPLC, and diethyl ether (Et_2O) were reagent grade and acquired from commercial sources (Sigma-Aldrich/Merck, Milano, Italy). Unless noted, all solvents were not anhydrous and used without further purification.

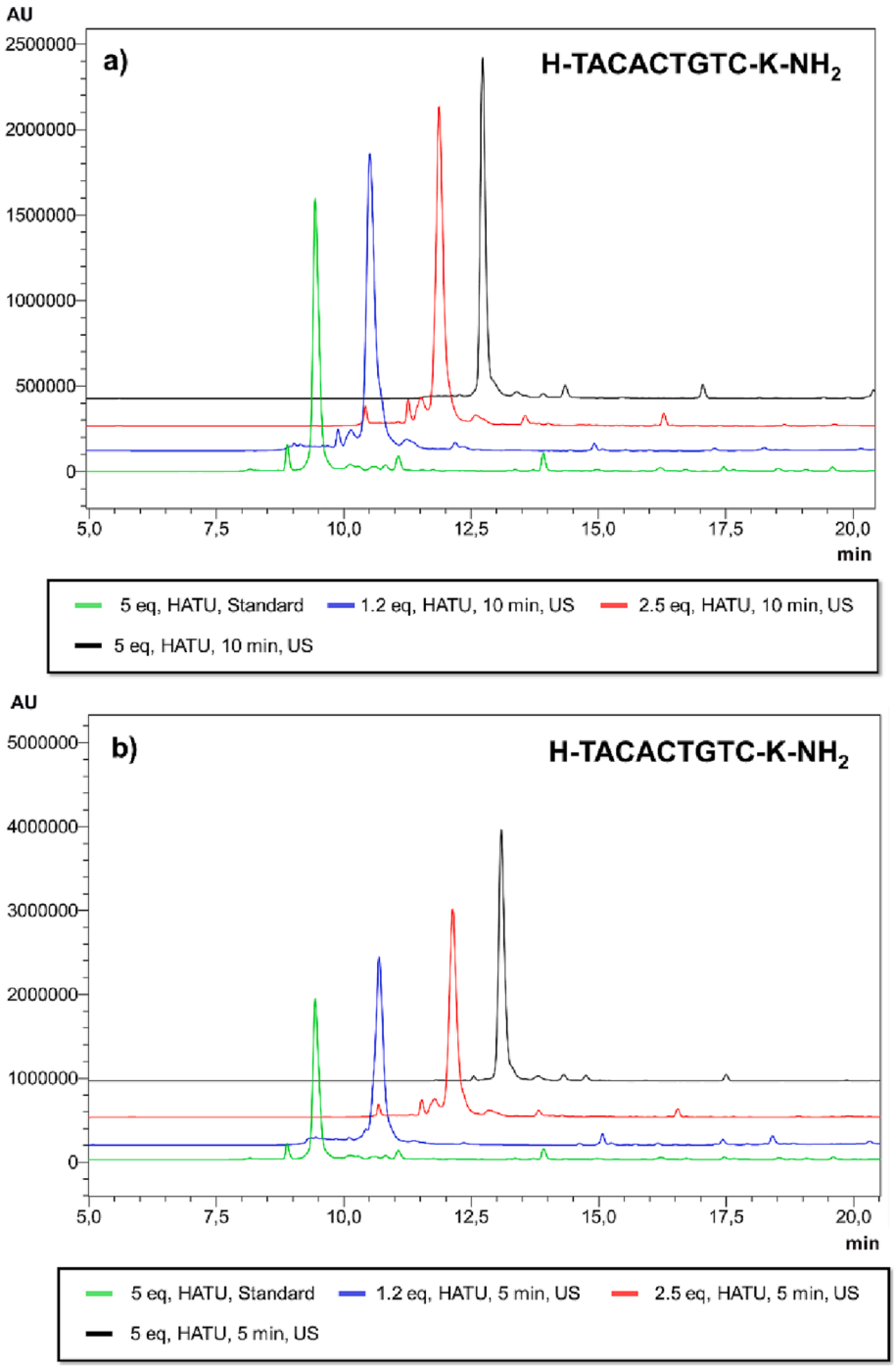

Fig. 9. Comparison of representative HPLC profiles of synthetic crudes of the 9-mer PNA oligomer (H-TACACTGTC-K-NH_2) obtained employing the same reagent excess at a) 10 min and b) 5 min reaction times. Equivalents of reagents and reaction times are indicated in the figure legend. The crude purity was calculated by integrating the peaks at t_R = 9.40 min [analytical HPLC gradient 2 in HPLC and Mass spectrometry procedures section].

4.1. HPLC and Mass spectrometry procedures

Analytical HPLC analyses were carried out by reverse-phase HPLC (Shimadzu Model SPD-40 V) on a Shim-pack GWS C18 column (150 mmL. × 4.6 mm I.D., 5 μm) with a flow rate of 1 mL/min, with detection at 220 and 260 nm wavelengths by a UV–Vis detector, and by using different elution gradients of MeCN (0.1 % TFA) in water (0.1 % TFA) [Gradient 1: isocratic H_2O (0.1 % TFA) over 2 min, 0–80% MeCN (0.1 % TFA) in H_2O (0.1% TFA) over 20 min; Gradient 2: isocratic H_2O (0.1 % TFA) over 2 min, 0–80% MeCN (0.1 % TFA) in H_2O (0.1 % TFA) over 15 min; Gradient 3: isocratic 10% MeCN (0.1 % TFA) in H_2O (0.1 % TFA) over 2 min, 10–60% MeCN (0.1 % TFA) in H_2O (0.1 % TFA) over 20 min]. Mass measurements were acquired by LC/MS system (LCMS-2020, Shimadzu) at the flow rate of 0.6 mL/min, and proton adducts, $[M + H]^+$, were used for empirical formula confirmation. Molecular weights of 23mer PNA were confirmed by Mass Spectrometry analyses, performed with a matrix-assisted laser desorption ionization time-of-flight (MALDI-TOF) microMX (Waters Co., Manchester, UK) mass spectrometer armed with a pulsed nitrogen laser (k = 337 nm).

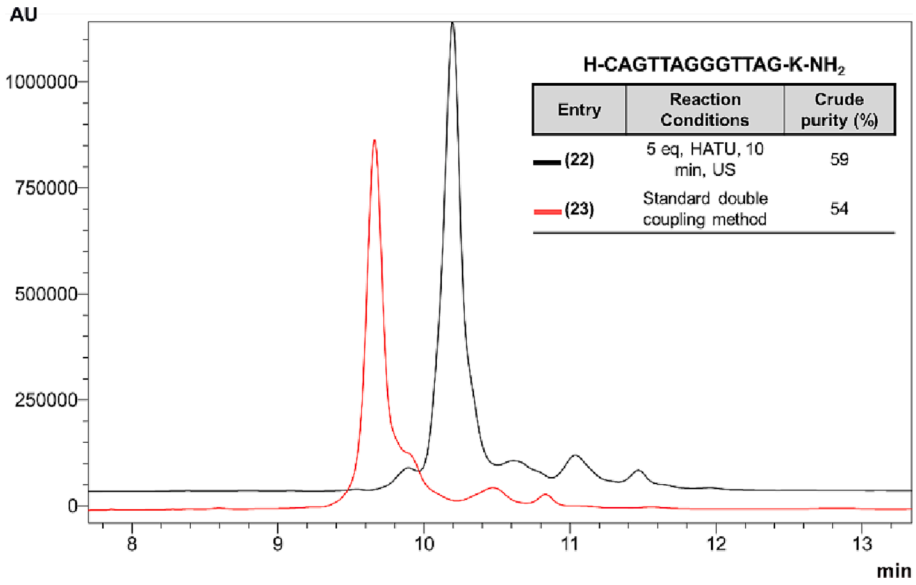

Fig. 10. Comparison of representative HPLC profiles of synthetic crudes of the TEL-13 PNA oligomer (H-CAGTTAGGGTTAG-K-NH_2). Equivalents of reagents and reaction times are indicated. The crude purity was calculated by integrating the peaks at $t_R = 9.66$ min, [analytical HPLC gradient 2 in HPLC and Mass spectrometry procedures section].

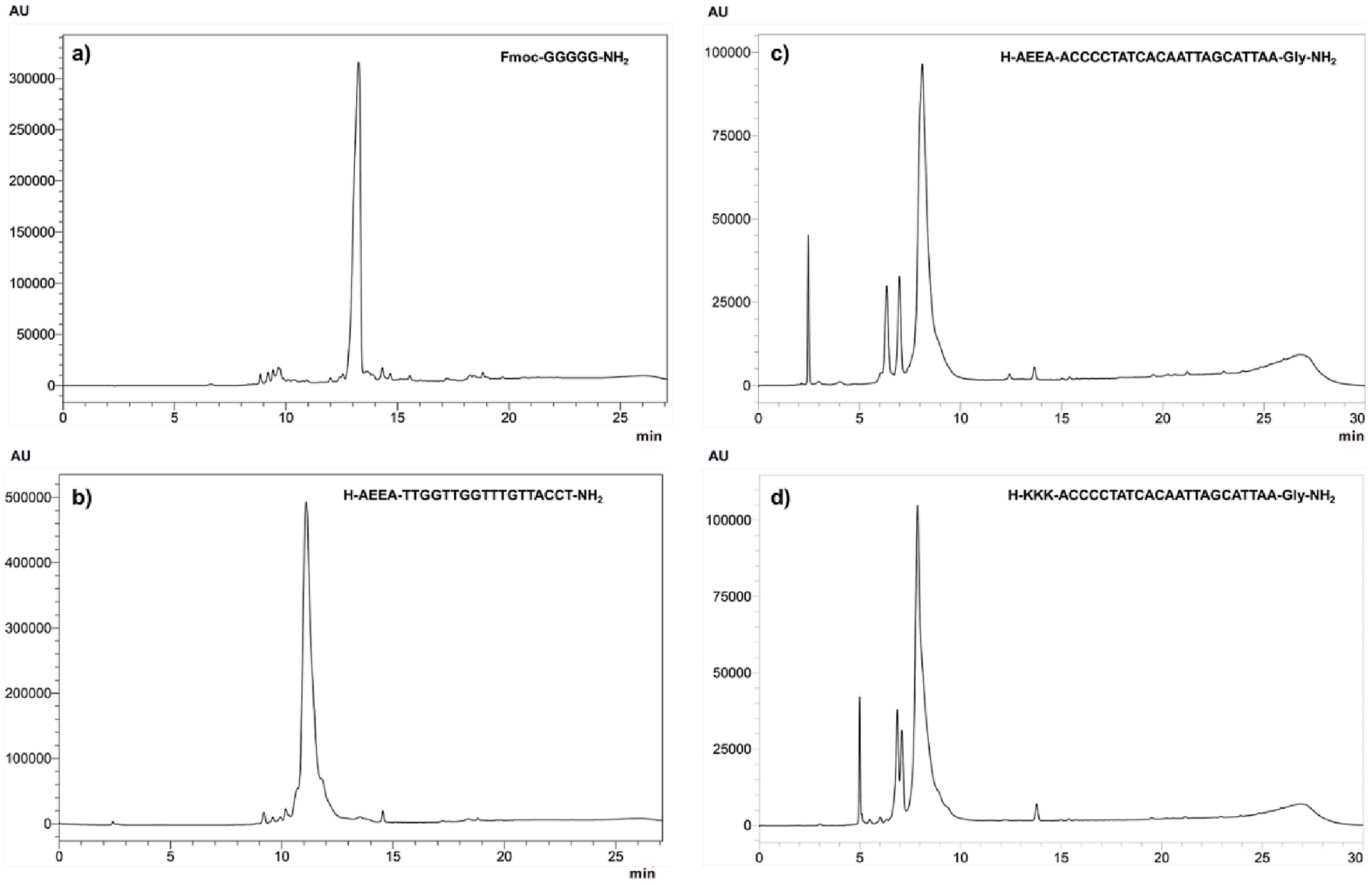

Fig. 11. HPLC profiles of a) 5- mer PNA (Fmoc-GGGGG-NH_2 $t_R = 13.3$ min) [analytical HPLC gradient 1 in HPLC and Mass spectrometry procedures section], b) 18-mer PNA (H-AEEA-TTGGTTGGTTTGTTACCT-Gly-NH_2 $t_R = 11.1$ min) [analytical HPLC gradient 2 in HPLC and Mass spectrometry procedures section], c) 23-mer PNA, H-AEEA-ACCCCTATCACAATTAGCATTAA-Gly-NH_2 $t_R = 8.46$ min and d) H-KKK-ACCCCTATCACAATTAGCATTAA-Gly-NH_2 $t_R = 8.48$ min and) [analytical HPLC Gradient 3 in HPLC and Mass spectrometry procedures section].

4.2. Support functionalization

Fmoc-Rink-Amide AM LL resin as solid support (1 g loading 0,2–0.45 mmol/g, 100–200 mesh as particle size) was placed into a 25 mL filtration column (ISOLUTE® SPE filtration column by Biotage, Uppsala, Sweden) provided with filter, stopper, and top cap. The pre-weight resin was swelled for 1 h in DMF and 30 min in DCM at RT on a shaker (Shaker Multi Reax P/N: 545–10000-00–2 by Heidolph, Schwabach, Germany). A vacuum manifold (CHROMABOND SPE by MACHEREY-NAGEL GmbH & Co. KG) was used for filtering the unreacted material after. The Fmoc group on the resin was removed by a 20 % piperidine/DMF solution (2 mL) under mechanical shaking (1 × 5 + 1 × 20 min). This step was monitored by observing a specific colorimetric test (the Kaiser test) for the presence of free primary amines. Fmoc-L-Lys(Boc)–OH (1.5 equiv, 161.7 mg) (for 5-,9- and 13 mer oligomers) and Fmoc-Gly-OH(1.5 equiv, 102.6 mg) (for 23-mer oligomers), HBTU (1.5 equiv, 130.9 mg)/HOBt (1.5 equiv, 52.8 mg) and DIPEA (3 equiv, 120 μL) were dissolved in DMF (2 mL), and added to the resin for the amino acid incorporation. The resulting mixture was reacted under mechanical shaking for 4 h at RT. Later, the resin was washed three times with DMF (2 mL each) and DCM (2 mL each). The unreacted amine groups were capped treating the resin for 15 min with a solution consisting of 0.5 M Ac_2O and 0.125 M DIPEA in DMF (2 mL). Finally, the solid support was washed and dried under a vacuum. Immediately before the Fmoc removal from the amino acid, 10 mg of dried Fmoc-L-Lys(Boc)- and Fmoc-Gly-bound resin was transferred into a 3 mL polypropylene tube equipped with a filter, stopper, and top cap. Then, the pre-swelled resin was treated with 1 mL of a 20 % piperidine/DMF solution and reacted under mechanical shaking for 7 min at rt. The resulting mixture was filtered in a 10 mL graduated flask and the filtrate was diluted to 10 mL with fresh DMF. 1 mL of 20% piperidine/DMF solution was employed as blank. A volume of 500 μL of the experimental solution was transferred to a UV quartz cell (3 × 10 mm) and placed in a UV–Vis spectrophotometer (Quartz cuvette with optical path length = 1 cm), and optical density was recorded at wavelengths ranging from 250 to 350 nm. Fulvene-piperidine adduct was monitored at 301 nm (extinction coefficient $\varepsilon = 7800\ mL \times mmol^{-1} \times cm^{-1}$). Finally, the Fmoc-loading quantification was extrapolated according to the formula: Fmoc-loading (mol/g) = [(Asample – Aref)/ε × l] × [10 mL/mg of resin]. Then, yield percentages were extrapolated by the formula: Fmoc-loading calcd/Starting Resin loading × 100.

4.3. Standard procedure

Fmoc-deprotection: 7 min (300uL). Coupling: PNA monomer equiv: 5 (Fmoc-PNA-T-OH 11.2 mg, Fmoc-PNA-C(Bhoc)–OH 15.5 mg, Fmoc-PNA-A(Bhoc)–OH 16.1 mg, Fmoc-PNA-G(Bhoc)–OH 16.5 mg); *HATU* (5 equiv, 8.55 mg); base solution (DIPEA 0.2 M, Lutidine 0.3 M); mechanical shaking at RT (30 min). Capping: 5 min with a solution (300 uL) consisting of 5% Ac2O and 6% lutidine in DMF.

4.4. Standard procedure at 45 °C

The same amounts of reactants were used as in the Standard Procedure: mechanical shaking at 45 °C (10 min). Capping: 5 min with a solution (300 uL) consisting of 5% Ac_2O and 6% lutidine in DMF.

4.5. Ultrasound SPS of PNA oligomers (US-PNAS)

The PNA synthesis was performed with cycles of amide bond formation (couplings), capping reaction, and *N*α-Fmoc removal reactions in an ultrasonic bath. An external thermometer was used to control the temperature between 25 and 30 °C during the different reaction steps.

4.6. US-PNAS procedure

5- and 9-mer and 13-mer PNA model oligomers were assembled with a 4,5 μmol scale on Fmoc-L-Lys(Boc)-Rink-Amide AM resin as solid support (25 mg, loading 0.18 mmol/g, 100–200 mesh as particle size). 23-mer oligomers were assembled with a 4,5 μmol scale on Fmoc-Gly-Rink-Amide AM resin as solid support (25 mg, loading 0.18 mmol/g, 100–200 mesh as particle size). After swelling the resin for 1 h, Fmoc-group was removed in the presence of a 20% piperidine/DMF solution by ultrasonic irradiation (1 + 0.5 min, 300 uL). After the deprotection step, the resin was washed three times with DMF (1 mL each) and DCM (1 mL each). Pre-activation of the PNA monomer was achieved in 300 μL DMF (only PNA-C was dissolved in 75% DMF and 25% DMSO), in the presence of different coupling reagents and base. The resulting reaction mixture was added to the resin and reacted by ultrasonication for the different coupling times before draining and washing. Next, a capping solution (300 μL) consisting of 5% Ac_2O and 6% lutidine in DMF was added to the reaction vessel and the reaction was performed by ultrasonic irradiation for 3 min. The successive PNA monomers were inserted by using the same protocol to obtain the desired sequence. Finally, the resin was washed and dried under vacuum.

The PNA oligomers were then removed from the resin by treating with TFA and *m*-cresol (95:5, 500 μL) for 3 h at rt under mechanical shaking, recovered by precipitation with cold Et_2O (1.5 mL), and then centrifuged three times (14600 rpm × 5 min). After removing the supernatant, the resulting white pellet was dried and then dissolved in water (0.1 %TFA)/acetonitrile (2:1, 1.5 mL) to be examined by reverse-phase HPLC and LC-MS.

4.7. Optimization of reaction conditions

All the PNA sequences were attained in triplicate. The amide reaction was achieved by adding to the resin the DMF solution containing pre-activated PNA monomer with the proper coupling reagent and base solution, by using one of the following protocols.

4.8. US-PNAS: Activating agent, 5 equiv, 10 min

a) Fmoc-deprotection: 0.5 + 1 min (300 μL). Coupling: PNA monomer equiv: 5 (Fmoc-PNA-T-OH 11.2 mg, Fmoc-PNA-C(Bhoc)–OH 15.5 mg, Fmoc-PNA-A(Bhoc)–OH 16.1 mg, Fmoc-PNA-G(Bhoc)–OH 16.5 mg); *HATU* (5 equiv, 8.55 mg); base solution (DIPEA 0.2 M, Lutidine 0.3 M); ultrasonic irradiation (10 min). Capping: 3 min (300 μL).
b) Fmoc-deprotection: 0.5 + 1 min (300 μL). Coupling: PNA monomer equiv: 5 (Fmoc-PNA-T-OH 11.2 mg, Fmoc-PNA-C(Bhoc)–OH 15.5 mg, Fmoc-PNA-A(Bhoc)–OH 16.1 mg, Fmoc-PNA-G(Bhoc)–OH 16.5 mg); *HBTU* (5 equiv, 8.53 mg): DIPEA (5 equiv, 4 μL); ultrasonic irradiation (10 min). Capping: 3 min (300 μL).
c) Fmoc-deprotection: 0.5 + 1 min (300 μL). Coupling: PNA monomer equiv: 5 (Fmoc-PNA-T-OH 11.2 mg, Fmoc-PNA-C(Bhoc)–OH 15.5 mg, Fmoc-PNA-A(Bhoc)–OH 16.1 mg, Fmoc-PNA-G(Bhoc)–OH 16.5 mg); *PYAOP* (5 equiv, 11.73 mg); DIPEA (5 equiv, 4 μL); ultrasonic irradiation (10 min). Capping: 3 min (300 μL).
d) Fmoc-deprotection: 0.5 + 1 min (300 μL). Coupling: PNA monomer equiv: 5 (Fmoc-PNA-T-OH 11.2 mg, Fmoc-PNA-C(Bhoc)–OH 15.5 mg, Fmoc-PNA-A(Bhoc)–OH 16.1 mg, Fmoc-PNA-G(Bhoc)–OH 16.5 mg), *DIC/OXYMA* (5 equiv 3.6 μL/3.2 mg); DIPEA (5 equiv, 4 μL); ultrasonic irradiation (10 min). Capping: 3 min (300 μL).
e) Fmoc-deprotection: 0.5 + 1 min (300 μL). Coupling: PNA monomer equiv: 5 (Fmoc-PNA-T-OH 11.2 mg, Fmoc-PNA-C(Bhoc)–OH 15.5 mg, Fmoc-PNA-A(Bhoc)–OH 16.1 mg, Fmoc-PNA-G(Bhoc)–OH 16.5 mg); *COMU* (5 equiv, 9.64 mg); DIPEA (5 equiv, 4 μL); ultrasonic irradiation (10 min). Capping: 3 min (300 μL).

4.9. US-PNAS: 4 equiv, 10 min

a) Fmoc-deprotection: 0.5 + 1 min (300 μL). Coupling: PNA monomer equiv: 4 (Fmoc-PNA-T-OH 9.1 mg, Fmoc-PNA-C(Bhoc)–OH 12.6 mg, Fmoc-PNA-A(Bhoc)–OH 13.1 mg, Fmoc-PNA-G(Bhoc)–OH 13.4 mg);

HATU (4 equiv, 6.84 mg); base solution (DIPEA 0.2 M, Lutidine 0.3 M); ultrasonic irradiation (10 min). Capping: 3 min (300 μL).

b) Fmoc-deprotection: 0.5 + 1 min (300 μL). Coupling: PNA monomer equiv: 4 (Fmoc-PNA-T-OH 9.1 mg, Fmoc-PNA-C(Bhoc)–OH 12.6 mg, Fmoc-PNA-A(Bhoc)–OH 13.1 mg, Fmoc-PNA-G(Bhoc)–OH 13.4 mg); *HBTU* (4 equiv, 6.83 mg); DIPEA (4 equiv, 3.2 μL); ultrasonic irradiation (10 min). Capping: 3 min (300 μL).

c) Fmoc-deprotection: 0.5 + 1 min. Coupling: PNA monomer equiv: 4 (Fmoc-PNA-T-OH 9.1 mg, Fmoc-PNA-C(Bhoc)–OH 12.6 mg, Fmoc-PNA-A(Bhoc)–OH 13.1 mg, Fmoc-PNA-G(Bhoc)–OH 13.4 mg); *PYAOP* (4 equiv, 2.35 mg); DIPEA (4 equiv, 3.2 μL); ultrasonic irradiation (10 min). Capping: 3 min.

4.10. US-PNAS: 3 equiv, 10 min

a) Fmoc-deprotection: 0.5 + 1 min (300 μL). Coupling: PNA monomer equiv: 3 (Fmoc-PNA-T-OH 6.8 mg, Fmoc-PNA-C(Bhoc)–OH 9.5 mg, Fmoc-PNA-A(Bhoc)–OH 9.8 mg, Fmoc-PNA-G(Bhoc)–OH 10.0 mg); coupling reagents (equiv): *HATU* (3 equiv, 5.13 mg); base solution (DIPEA 0.2 M, Lutidine 0.3 M); ultrasonic irradiation (10 min). Capping: 3 min (300 μL).

15 4.11 US-PNAS: 2 equiv, 10 min

a) Fmoc-deprotection: 0.5 + 1 min (300 μL). Coupling: PNA monomer equiv: 2 (Fmoc-PNA-T-OH 4.6 mg, Fmoc-PNA-C(Bhoc)–OH 6.3 mg, Fmoc-PNA-A(Bhoc)–OH 6.5 mg, Fmoc-PNA-G(Bhoc)–OH 6.7 mg); coupling reagents (equiv): *HATU* (2 equiv, 3.42 mg); base solution (DIPEA 0.2 M, Lutidine 0.3 M); ultrasonic irradiation (10 min). Capping: 3 min (300 μL).

4.12. US-PNAS: HATU, 5 equiv, 5 min

Fmoc-deprotection: 0.5 + 1 min (300 μL). Coupling: PNA monomer equiv: 5 (Fmoc-PNA-T-OH 11.2 mg, Fmoc-PNA-C(Bhoc)–OH 15.5 mg, Fmoc-PNA-A(Bhoc)–OH 16.1 mg, Fmoc-PNA-G(Bhoc)–OH 16.5 mg); *HATU* (5 equiv, 8.55 mg); base solution (DIPEA 0.2 M, Lutidine 0.3 M); ultrasonic irradiation (5 min). Capping: 3 min (300 μL).

4.13. US-PNAS: HATU, 2.5 equiv, 10 min

Fmoc-deprotection: 0.5 + 1 min (300 μL). Coupling: PNA monomer equiv: 2.5 (Fmoc-PNA-T-OH 5.7 mg, Fmoc-PNA-C(Bhoc)–OH 7.9 mg, Fmoc-PNA-A(Bhoc)–OH 8.2 mg, Fmoc-PNA-G(Bhoc)–OH 8.4 mg); coupling reagents (equiv): *HATU* (2.5 equiv, 4.23 mg); base solution (DIPEA 0.2 M, Lutidine 0.3 M); ultrasonic irradiation (10 min). Capping: 3 min (300 μL).

4.14. US-PNAS: HATU, 2.5 equiv, 5 min

Fmoc-deprotection: 0.5 + 1 min (300 μL). Coupling: PNA monomer equiv: 2.5 (Fmoc-PNA-T-OH 5.7 mg, Fmoc-PNA-C(Bhoc)–OH 7.9 mg, Fmoc-PNA-A(Bhoc)–OH 8.2 mg, Fmoc-PNA-G(Bhoc)–OH 8.4 mg); coupling reagents (equiv): *HATU* (2.5 equiv, 4.23 mg); base solution (DIPEA 0.2 M, Lutidine 0.3 M); ultrasonic irradiation (5 min). Capping: 3 min (300 μL).

4.15. US-PNAS: HATU, 1.2 equiv, 10 min

Fmoc-deprotection: 0.5 + 1 min (300 μL). Coupling: PNA monomer equiv: 1.2 (Fmoc-PNA-T-OH 2.9 mg, Fmoc-PNA-C(Bhoc)–OH 4.0 mg, Fmoc-PNA-A(Bhoc)–OH 4.1 mg, Fmoc-PNA-G(Bhoc)–OH 4.2 mg); coupling reagents (equiv): *HATU* (1.2 equiv, 2.1 mg); base solution (DIPEA 0.2 M, Lutidine 0.3 M); ultrasonic irradiation (10 min). Capping: 3 min (300 μL).

4.16. US-PNAS: HATU, 1.2 equiv, 5 min

Fmoc-deprotection: 0.5 + 1 min (300 μL). Coupling: PNA monomer equiv: 1.2 (Fmoc-PNA-T-OH 2.9 mg, Fmoc-PNA-C(Bhoc)–OH 4.0 mg, Fmoc-PNA-A(Bhoc)–OH 4.1 mg, Fmoc-PNA-G(Bhoc)–OH 4.2 mg); coupling reagents (equiv): *HATU* (1.2 equiv, 2.1 mg); base solution (DIPEA 0.2 M, Lutidine 0.3 M); ultrasonic irradiation (5 min). Capping: 3 min (300 μL).

Funding

This research was funded by MIUR, PRIN 2017 (2017PHRC8X_004) and PON R&I 2014-2020-AIM (Attraction and International Mobility), project AIMs-2, linea 1.

CRediT authorship contribution statement

Alessandra Del Bene: Data curation. **Antonia D'Aniello: . Stefano Tomassi:** Data curation. **Francesco Merlino: . Vincenzo Mazzarella: . Rosita Russo:** Data curation. **Angela Chambery:** Data curation. **Sandro Cosconati:** Writing – review & editing. **Salvatore Di Maro:** Conceptualization, Data curation, Writing – review & editing, Supervision. **Anna Messere:** Conceptualization, Data curation, Writing – review & editing, Supervision.

Declaration of Competing Interest

The authors declare that they have no known competing financial interests or personal relationships that could have appeared to influence the work reported in this paper.

Appendix A. Supplementary data

Supplementary data to this article can be found online at https://doi.org/10.1016/j.ultsonch.2023.106360.

References

[1] P.E. Nielsen, M. Egholm, R.H. Berg, O. Buchardt, Sequence-selective recognition of DNA by strand displacement with a thymine-substituted polyamide, Science 254 (1991) 1497–1500, https://doi.org/10.1126/science.1962210.

[2] J. Saarbach, P.M. Sabale, N. Winssinger, Peptide nucleic acid (PNA) and its applications in chemical biology, diagnostics, and therapeutics Curr, Opin. Chem. Biol. 52 (2019) 112–124, https://doi.org/10.1016/j.cbpa.2019.06.006.

[3] S. Siddiquee, K. Rovina A. Azriah, Review of Peptide Nucleic Acid Adv. Technol. Bio. Med. 03 (2015) 1−10 https://doi.org/10.4172/2379-1764.1000131.

[4] P.E. Nielsen, Sequence-selective DNA recognition by synthetic ligands Bioconjug, Chem 2 (1991) 1–12, https://doi.org/10.1021/bc00007a001.

[5] B.A. Armitage, The impact of nucleic acid secondary structure on PNA hybridization, Drug Discov Today 8 (2003) 222–228, https://doi.org/10.1016/S1359-6446(03)02611-4.

[6] K.R. Singh, P. Sridevi, R.P. Singh, Potential applications of peptide nucleic acid in biomedical domain, Eng Rep 12238 (2020), https://doi.org/10.1002/eng2.12238.

[7] C.D. Pesce, F. Bolacchi, B. Bongiovanni, F. Cisotta, M. Capozzi, S. Diviacco, F. Quadrifoglio, R. Mango, G. Novelli, G. Mossa, C. Esposito, D. Ombres, G. Rocchi, A. Bergamini, Anti-gene peptide nucleic acid targeted to proviral HIV-1 DNA inhibits in vitro HIV-1 replication Antiviral Research, Antiviral Res. 66 (2005) 13–22, https://doi.org/10.1016/j.antiviral.2004.12.001.

[8] F. Rigo, Y. Hua, A.R. Krainer, C.F. Bennett, Antisense-based therapy for the treatment of spinal muscular atrophy, J. Cell. Biol. 199 (2012) 21–25, https://doi.org/10.1083/jcb.201207087.

[9] J.C. Wu, Q.C. Meng, H.M. Ren, H.T. Wang, J. Wu, Q. Wang, Recent advances in peptide nucleic acid for cancer bionanotechnology, Acta Pharmacol Sin. 38 (2017) 798–805, https://doi.org/10.1038/aps.2017.33.

[10] K. Maekawa, M. Azuma, Y. Okuno, T. Tsukamoto, K. Nishiguchi, K. Setsukinai, H. Maki, Y. Numata, H. Takemoto, M. Rokushima, Antisense peptide nucleic acid–peptide conjugates for functional analyses of genes in Pseudomonas aeruginosa, Bioorg Med. Chem. 23 (2015) 7234–7239, https://doi.org/10.1016/j.bmc.2015.10.020.

[11] H. Wang, Y. He, Y. Xia, L. Wang, S. Liang, Inhibition of gene expression and growth of multidrug-resistant Acinetobacter baumannii by antisense peptide nucleic acids, Mol. Biol. Rep. 41 (2014) 7535–7541, https://doi.org/10.1007/s11033-014-3643-2.

[12] Z. Zeng, S. Han, W. Hong, Y. Lang, F. Li, Y. Liu, Z. Li, Y. Wu, W. Li, X. Zhang, Z. Cao, A Tat-conjugated Peptide Nucleic Acid Tat-PNA-DR Inhibits Hepatitis B Virus Replication in Vitro and In vivo by targeting LTR direct repeats of HBV RNA, Mol. Ther. Nucleic Acids 5 (2016) e295.

[13] U. Koppelhus, S. K. Awasthi, V. Zachar, H. U. Holst, P., Ebbesen, P. E. Nielsen, Cell-Dependent Differential Cellular Uptake of PNA, Peptides, and PNA-Peptide Conjugates, Antisense Nucleic Acid Drug Dev. 12 (2002) 51−63, 10.1089/108729002760070795.

[14] S. Abes, J.J. Turner, G.D. Ivanova, D. Owen, D. Williams, A. Arzumanov, P. Clair, M.J. Gait, B. Lebleu, Efficient splicing correction by PNA conjugation to an R6-Penetratin delivery peptide, Nucleic Acids Res. 35 (2007) 4495–4502, https://doi.org/10.1093/nar/gkm418.

[15] G. Milano, D. Musumeci, M. Gaglione, Messere, A, An alternative strategy to synthesize PNA and DNA magnetic conjugates forming nanoparticle assembly based on PNA/DNA duplexes, Mol BioSyst. 6 (2010) 553–561, https://doi.org/10.1039/B915680A.

[16] M. Gaglione, G. Milano, A. Chambery, L. Moggio, A. Romanelli, A. Messere, PNA-based artificial nucleases as antisense and anti-miRNA oligonucleotide agents, Mol BioSyst. 7 (2011) 2490–2499, https://doi.org/10.1039/C1MB05131H.

[17] A. Gupta, A. Mishra, N. Puri, Peptide nucleic acids: Advanced tools for biomedical applications, J. Biotechnol. 259 (2017) 148–159, https://doi.org/10.1016/j.jbiotec.2017.07.026.

[18] E. Uhlmann, A. Peyman, G. Breipohl, D. W. Will, PNA: Synthetic Polyamide Nucleic Acids with Unusual Binding Properties, Angew. Chem., Int. Ed. 37 (1998) 2796–2823, 10.1002/(sici)1521-3773(19981102)37:20%3C2796::aid-anie2796%3E3.0.co;2-k.

[19] L. Bialy, J.J. Diaz-Mochon, E. Specker, L. Keinicke, M. Bradley, Dde-protected PNA monomers, orthogonal to Fmoc, for the synthesis of PNA-peptide conjugates, Tetrahedron 61 (2005) 8295–8305, https://doi.org/10.1016/j.tet.2005.06.003.

[20] F. Wojciechowski, R.H. Hudson, A Convenient Route to N-[2-(Fmoc)aminoethyl] glycine Esters and PNA Oligomerization Using a Bis-N-Boc Nucleobase Protecting Group Strategy, J. Org. Chem. 73 (2008) 3807–3816, https://doi.org/10.1021/jo800195j.

[21] Z.C. Liu, D.S. Shin, K.T. Lee, B.H. Jun, Y.K. Kim, Y.S. Lee, Synthesis of photolabile o-nitroveratryloxycarbonyl (NVOC) protected peptide nucleic acid monomers, Tetrahedron 61 (2005) 7967–7973, https://doi.org/10.1016/j.tet.2005.06.002.

[22] F. Debaene, N. Winssinger, Azidopeptide Nucleic Acid. An Alternative Strategy for Solid-Phase Peptide Nucleic Acid (PNA) Synthesis, Org. Lett. 5 (2003) 4445–4447, https://doi.org/10.1021/ol0358408.

[23] D. Musumeci, G.N. Roviello, M. Valente, R. Sapio, C. Pedone, E.M. Bucci, New synthesis of PNA-3'DNA linker monomers, useful building blocks to obtain PNA/DNA chimeras, Biopolymers 76 (2004) 535–542, https://doi.org/10.1002/bip.20135.

[24] D. Capasso, L. De Napoli, G. Di Fabio, A. Messere, D. Montesarchio, C. Pedone, G. Piccialli, M. Saviano, Solid phase synthesis of DNA-3′-PNA chimeras by using Bhoc/Fmoc PNA monomers, Tetrahedron 57 (2001) 9481–9486, https://doi.org/10.1016/S0040-4020(01)00944-9.

[25] A.Y. Shaikh, A.M. Hansen, H. Franzyk, Fmoc-Based Assembly of PNA Oligomers: Manual and Microwave-Assisted Automated Synthesis, Methods Mol Biol. 2020 (2015) 1–16, https://doi.org/10.1007/978-1-0716-0243-0_1.

[26] M. Egholm, R. A. Casale, In Solid-phase Synthesis; S. A. Kates, F. Albericio, Eds.; Dekker: New York, 2000; pp 549–578, 10.1201/9781482270303.

[27] F. Altenbrunn, O. Seitz, O-Allyl protection in the Fmoc-based synthesis of difficult PNA, Org. Biomol. Chem. 6 (2008) 2493–2498, https://doi.org/10.1039/B805165H.

[28] R. Joshi, D. Jha, W. Su, J. Engelmann, Facile synthesis of peptide nucleic acids and peptide nucleic acid-peptide conjugates on an automated peptide synthesizer, J. Pept. Sci. 17 (2011) 8–13, https://doi.org/10.1002/psc.1305.

[29] R. Pipkorn, S. Rawer, M. Wiessler, W. Waldeck, M. Koch, H.H. Schrenk, K. Braun, SPPS resins impact the PNA-syntheses' improvement, Int. J. Med. Sci. 10 (2013) 331–337. https://www.medsci.org/v10p0331.htm.

[30] C. Avitabile, L. Moggio, L.D. D'Andrea, C. Pedone, A. Romanelli, Development of an efficient and low-cost protocol for the manual PNA synthesis by Fmoc chemistry, Tetrahedron Lett. 51 (29) (2010) 3716–3718, https://doi.org/10.1016/j.tetlet.2010.05.026.

[31] H. Lee, J.H. Jeon, J.C. Lim, H. Choi, Y. Yoon, S.K. Kim, Peptide Nucleic Acid Synthesis by Novel Amide Formation, Org. Lett. 9 (2007) 3291–3293, https://doi.org/10.1021/ol071215h.

[32] K. Gogoi, M.V. Mane, S.S. Kunte, V.A. Kumar, A versatile method for the preparation of conjugates of peptides with DNA/PNA/analog by employing chemo-selective click reaction in water, Nucleic Acids Res. 35 (2007) e139.

[33] C. Li, A.J. Callahan, K.S. Phadke, B. Bellaire, C.E. Farquhar, G. Zhang, C.K. Schissel, A.J. Mijalis, N. Hartrampf, A. Loas, D.E. Verhoeven, B.L. Pentelute, Automated Flow Synthesis of Peptide–PNA Conjugates, ACS Cent. Sci. 8 (2022) 205–213, https://doi.org/10.1021/acscentsci.1c01019.

[34] F. Merlino, S. Tomassi, A.M. Yousif, A. Messere, L. Marinelli, P. Grieco, E. Novellino, S. Cosconati, S. Di Maro, Boosting Fmoc Solid-Phase Peptide Synthesis by Ultrasonication, Org. Lett. 21 (2019) 6378–6382, https://doi.org/10.1021/acs.orglett.9b02283.

[35] S. Tomassi, M.P. Dimmito, M. Cai, A. D'Aniello, A. Del Bene, A. Messere, Z. Liu, T. Zhu, V.J. Hruby, A. Stefanucci, S. Cosconati, A. Mollica, S. Di Maro. CLIPSing Melanotan-II to Discover Multiple Functionally Selective hMCR Agonists, J. Med. Chem., 65, (2022), 4007-4017, https://doi:10.1021/acs.jmedchem.1c01848.

[36] S. Tomassi, A.M. Trotta, C. Ieranò, F. Merlino, A. Messere, G. Rea, F. Santoro, D. Brancaccio, A. Carotenuto, V.M. D'Amore, F.S. Di Leva, E. Novellino, S. Cosconati, L. Marinelli, S. Scala, S. Di Maro, Disulfide Bond Replacement with 1,4- and 1,5-Disubstituted [1,2,3]-Triazole on C-X-C Chemokine Receptor Type 4 (CXCR4) Peptide Ligands: Small Changes that Make Big Differences, Chem. Eur. J. 26 (2020) 10113–10125, https://doi.org/10.1002/chem.202002468.

[37] G. Wołczański, H. Płóciennik, M. Lisowski, P. Stefanowicz, A faster solid phase peptide synthesis method using ultrasonic agitation, Tetrahedron Lett. 60 (2019) 1814–1818, https://doi.org/10.1016/j.tetlet.2019.05.069.

[38] S.J. Raheem, B.W. Schmidt, V.R. Solomon, A.K. Salih, E.W. Price, Ultrasonic-Assisted Solid-Phase Peptide Synthesis of DOTA-TATE and DOTA-linker-TATE Derivatives as a Simple and Low-Cost Method for the Facile Synthesis of Chelator-Peptide Conjugates, Bioconjug. Chem. 32 (2021) 1204–1213, https://doi.org/10.1021/acs.bioconjchem.0c00325.

[39] R. D. M. Silva, J. F. Machado, K. Gonçalves, F.M. Lucas, S. Batista, R. Melo, T.S Morais, J.D.G. Correia, Ultrasonication Improves Solid Phase Synthesis of Peptides Specific for Fibroblast Growth Factor Receptor and for the Protein-Protein Interface RANK-TRAF6, Molecules, 26, (2021), 7349-7358, 10.3390/molecules26237349.

[40] G. Cravotto, P. Cintas, Power ultrasound in organic synthesis: moving cavitational chemistry from academia to innovative and large-scale applications, Chem. Soc. Rev. 35 (2006) 180–196, https://doi.org/10.1039/B503848K.

[41] B. Banerjee, Recent developments on ultrasound assisted catalyst-free organic synthesis, Ultrasonics Sonochem., 35, Part A (2017) 1–14, https://doi.org/10.1016/j.ultsonch.2016.09.023.

[42] M. Lupacchini, A. Mascitti, G. Giachi, L. Tonucci, N. d'Alessandro, J. Martinez, E. Colacino, Sonochemistry in non-conventional, green solvents or solvent-free reactions, Tetrahedron 73 (2017) 609–653, https://doi.org/10.1016/j.tet.2016.12.014.

[43] A.A. Kiss, R. Geertman, M. Wierschem, M. Skiborowski, B. Gielen, J. Jordens, J. J. John, T. V, Gerven, Ultrasound-assisted emerging technologies for chemical processes, J. Chem. Technol. Biotechnol. 93 (2018) 1219–1227, https://doi.org/10.1002/jctb.5555.

[44] E.I. Vrettos, N. Sayyad, E.M. Mavrogiannaki, E. Stylos, K.D. Androniki, S. Papas, T. Mavromoustakos, V. Theodorou, A.G. Tzakos, Unveiling and tackling guanidinium peptide coupling reagent side reactions towards the development of peptide-drug conjugates, RSC Adv. 7 (2017) 50519–50526, https://doi.org/10.1039/C7RA06655D.

[45] M.R. Jackson, B.M. Bavelaar, P.A. Waghorn, M.R. Gill, A.H. El-Sagheer, T. Brown, M. Tarsounas, K.A. Vallis, Radiolabeled Oligonucleotides Targeting the RNA Subunit of Telomerase Inhibit Telomerase and Induce DNA Damage in Telomerase-Positive Cancer Cells, Cancer. Res. 79 (2019) 4627–4637, https://doi.org/10.1158/0008-5472.CAN-18-3594.

[46] M.M. Fabani, C. Abreu-Goodger, D. Williams, P.A. Lyons, A.G. Torres, K.G. Smith, A.J. Enright, M.J. Gait, E. Vigorito, Efficient inhibition of miR-155 function in vivo by peptide nucleic acids, Nucleic Acids Res. 38 (2010) 4466–4475, https://doi.org/10.1093/nar/gkq160.

[47] R. Bahal, B. Sahu, S. Rapireddy, C.-M. Lee, D.H. Ly, Sequence-Unrestricted, Watson-Crick Recognition of Double Helical B-DNA by (R)-MiniPEG-γPNAs, Chembiochem 13 (2012) 56–60, https://doi.org/10.1002/cbic.201100646.

[48] B. Sahu, V. Chenna, K.L. Lathrop, S.M. Thomas, G. Zon, K.J. Livak, D.H. Ly, Synthesis of Conformationally Preorganized and Cell-Permeable Guanidine-Based ɣ-Peptide Nucleic Acids (ɣGPNAs), J. Org. Chem. 74 (2009) 1509–1516, https://doi.org/10.1021/jo802211n.

[49] M.K. Gupta, B.R. Madhanagopal, D. Datta, K.N. Ganesh, Structural Design and Synthesis of Bimodal PNA That Simultaneously Binds Two Complementary DNAs To Form Fused Double Duplexes, Org. Lett. 22 (2020) 5255–5260, https://doi.org/10.1021/acs.orglett.0c01950.

[50] P. Bhingardeve, B.R. Madhanagopal, K.N. Ganesh, Cγ(S/R)-Bimodal Peptide Nucleic Acids (Cγ-bm-PNA) Form Coupled Double Duplexes by Synchronous Binding to Two Complementary DNA Strands, J. Org. Chem. 85 (2020) 13680–13693, https://doi.org/10.1021/acs.joc.0c01853.

[51] A. Gorai, R. Chaudhuri, T.K. Mukhopadhyay, A. Datta, J. Dash, Thiazole Containing PNA Mimic Regulates c-MYC Gene Expression through DNA G-Quadruplex, Bioconjug. Chem. 33 (2022) 1145–1155, https://doi.org/10.1021/acs.bioconjchem.2c00075.